Cytometry 24:214–225 (1996)

A Strategy for Multiple Immunophenotyping by Image Cytometry: Model Studies Using Latex Microbeads Labeled With Seven Streptavidin-Bound Fluorochromes

André Gothot, Jean-Claude Grosdent, and Jean-Michel Paulus
Laboratory of Hematology, Hôpital du Sart-Tilman and University of Liège, Liège, Belgium

Received for publication October 11, 1995; accepted February 19, 1996

Multiple immunophenotyping is aimed at identifying several cell populations in a single labeling procedure by their ability to bind combinations of specific labeled antibodies. The present work demonstrates the simultaneous discrimination by using image cytometry of aminomethylcoumarin acetate (AMCA), Lucifer yellow (LY), fluorescein isothiocyanate (FITC), R-phycoerythrin (PE), PE-Texas red tandem (Red613), peridinin-chlorophyll protein (PerCP), and allophycocyanin (APC), which were all bound to latex beads as streptavidin-conjugated fluorochromes. This has been the result of a step-by-step optimization of the several factors affecting the sensitivity and specificity of multiple immunofluorescence analysis. First, 14 streptavidin-conjugated fluorochromes were evaluated by using spectrofluorometry. A primary selection was then made of ten spectrally separable dyes that could be evaluated by using image cytometry. These dyes were bound to latex particles, and specific filter combinations were assembled to minimize crosstalk between fluorophores while preserving sufficient fluorescence intensity and counting statistics. Potential probe associations were then assessed by measuring the emissions of all fluorochromes that were detected by each filter combination. The resulting crosstalk matrix served as the basic tool both for final selection of the optimal filter combination and for dye set (composed, in this case, of the seven fluorochromes described above) and for mathematical correction of residual spectral overlap. Next, an image cytometry system was adapted to collect seven images of matched brightness with the selected combination of excitation/emission filters and dichroic mirrors. Finally, seven-parameter synthetic images were generated by digital image processing. © 1996 Wiley-Liss, Inc.

Key terms: Multiple immunophenotyping, image cytometry, multicomponent analysis, spectral compensation

Multiple fluorescence immunophenotyping allows the determination of several target antigens on individual cells by using fluorochrome-labeled antibodies. Thus far, double and triple immunophenotyping has been used extensively, for instance, to characterize hemopoietic precursor subpopulations (9,11,17,18,36) and to investigate aberrant antigen combinations expressed by leukemic blasts (5). Recent works have demonstrated the feasibility of discriminating four (13,18,19,22,23,32,33) or five (4,8,27,38) fluorescence signals by using flow or image cytometry. However, to detect rare or complex phenotypes, there is still a need to devise methods for the discrimination of greater numbers of probes bound to individual cells. The development of multiple immunophenotyping has benefitted from the availability of monoclonal antibodies that bind to precursor subpopulations (7,28), from the introduction of sets of fluorochromes spanning a wide region of the light spectrum (see references in Table 1), and from recent studies on the theory and application of multiparameter imaging (3,8,12,33,38). Moreover, further improvements of such procedures can be provided by technological advances in fluorescence microscopy and digital image processing.

Our initial motivation in developing multiple immunophenotyping color analysis has been to help classify early hemopoietic precursors and progenitors and to de-

Supported by grants from the FNRS (3.4562.85 and 3.4502.86), the Loterie Nationale Belge, Télévie (7.4545.92), the Fonds de la Recherche of the University of Liège, and the Oeuvre Belge du Cancer.

A.G. and J.M.P. are Aspirant and Director of Research, respectively, at the Fonds National de la Recherche Scientifique (FNRS), Brussels, Belgium.

Address reprints requests to Jean-Michel Paulus, Laboratory of Hematology, Hôpital du Sart-Tilman, 4000 Liège, Belgium.

termine their pathways of development. Because an informative phenotype of hemopoietic precursors should ideally specify both the lineage specificity and the stage of maturation, we estimated that the simultaneous detection of six to eight antigens would be required to enumerate uncommitted stem cells and progenitors committed to the granulomonocytic, erythrocytic, thrombocytic, and lymphocytic lineages. In leukemia diagnosis, multiple immunophenotyping could be exploited to improve the detection of aberrant antigenic phenotypes expressed by leukemic blasts.

A major problem in multicolor fluorescence applications is spectral overlap. Because of the broad excitation and/or emission spectra of available fluorochromes, the optimal emission band of each dye generally collects the light emitted by more than one component of the labeling cocktail. This fraction of the emission of a given fluorochrome, which is collected through an adjacent filter set, is termed spectral overlap. When more than four dyes are mixed, spectral overlap has to be corrected by mathematical rather than electronic compensation (3,30). However, the accuracy of spectral correction based on multicomponent analysis depends on many factors, such as the fluorescence spectra of individual components, the selected excitation/emission bands, as well as a number of optical and electronic variables (24). Therefore, a thorough and exhaustive examination of these variables is needed. In this paper, 14 streptavidin-conjugated fluorochromes were first evaluated by spectrofluorometry. From this evaluation, an initial set of ten spectrally separable dyes and filter combinations were chosen. These dyes were then bound to latex particles, and the various parameters influencing the accuracy of multiple immunophenotyping were assessed by measuring the emission of all dyes in each filter combination. The resulting crosstalk matrix served as the basic tool for final selection of the optimal probe and filter associations, for development of the image cytometry set up, and for correction of residual spectral overlap. The present study illustrates the application of this strategy to the discrimination of seven protein-conjugated dyes bound to latex particles.

MATERIALS AND METHODS

Fluorescent Conjugates and Microbeads

Because fluorescence immunophenotyping measures the emission of protein-bound fluorochromes, all of the model studies described below used streptavidin (SA)-fluorochrome conjugates rather than free dyes. SA-conjugates of Cascade blue (CB), Lucifer yellow (LY), Bodipy, fluorescein isothiocyanate (FITC), R-phycoerythrin (PE), Texas red (TxR), and allophycocyanine (APC) were obtained from Molecular Probes (Eugene, OR). SA-conjugates of tandem labels of PE and TxR (Red613) and PE and Cy5 (Red670) were purchased from Gibco BRL (Grand Island, NY). Peridinin-chlorophyll-protein complex conjugated to SA (PerCP) was from Becton-Dickinson (Mountain View, CA); aminomethylcoumarin acetate-SA (AMCA), cyanin 3-SA (Cy3), and cyanin 5-SA (Cy5) were from Jackson Immunoresearch (West Grove, PA). C-phycocyanin-SA (CPC) was purchased from Sigma (St. Louis, MO) (Table 1).

Table 1
Spectrofluorometric Data of 14 Dyes Evaluated for Multiple Labeling

Fluorochrome[a]	Excitation max. (nm)	Emission max. (nm)	References
AMCA	345	450	2,16,40
CB	379	420	40
LY	424	533	6,35
FITC	493	531	26
Bodipy	500	513	14
PE	563	576	10,21
Cy3	554	571	31
Red613	565	613	39
TxR	593	614	37
PerCP	493	675	1
Red670	540	666	39
APC	653	660	10,21
CPC	629	643	10,21
Cy5	658	668	31

[a]All fluorescence measurements were performed on solutions of streptavidin-conjugated fluorochromes. For fluorochrome abbreviations, see Materials and Methods.

To simulate cell surfaces labeled with fluorescent antibodies, Accuscan synthetic microbeads (Sigma), which have surfaces linked covalently with goat antimouse immunoglobulin (IgG), were used as model particles. Their mean diameter, as measured by image cytometry, was 10.61 μm with a coefficient of variation (CV) of 4.8%, and their mean cross-sectional area was 88.61 μm^2 with a CV of 9.8%. They were sequentially incubated with mouse biotinylated IgG (Molecular Probes) at various concentrations for 1 h at 4°C and with SA-conjugated fluorochromes for 30 min at 4°C.

Spectrofluorometry

Excitation and emission spectra were obtained in an LS 50 Perkin Elmer spectrofluorometer. Fluorescence measurements were performed on solutions of streptavidin-conjugated dyes diluted in phosphate-buffered saline (PBS) containing 0.2% bovine serum albumin (BSA). Emission spectra were corrected for the spectral characteristics of source, monochromators, and photomultipliers of the spectrofluorometer according to the procedure recommended by the manufacturer. Briefly, correction factors between 400 and 630 nm were obtained by comparing the emission spectrum of quinine sulphate, which was used as standard compound, with its corrected spectrum. Assuming that the wavelength-dependent efficiency of the detection system remained constant above 630 nm, a monotonous correction using the 630 nm correction factor was applied between 630 and 800 nm.

Fluorescence Microscopy

The microscope instrumentation is shown in Figure 1. An Axiovert 135 inverted microscope (Zeiss, Ober-

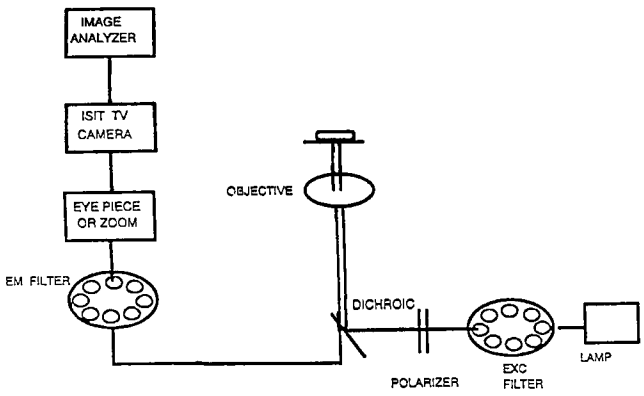

FIG. 1. Schematic representation of the image cytometry setup. Note that the same lenses serve as both objective and condenser.

kochen, Federal Republic of Germany) was equipped with a 100 W high-pressure mercury lamp. A 75 W Xenon lamp was mounted on a second port on the same microscope. It was not used in this study, because its intensity did not match that of the mercury lamp, except in the 450–540 nm range (34), where, however, the mercury lamp provided sufficient excitation for FITC, PE, Red613, and PerCP. Latex particles were suspended in a drop of saline solution and examined on a 0.17-μm-thick Hamax slide (Biotest, Brussels, Belgium). A ×40 oil NA 1.3 Plan Neofluar objective obtained from Zeiss was used in all experiments together with a ×1.0 camera ocular lens. High numerical aperture maximized light gathering of fluorescence emission and signal-to-noise ratio while minimizing the influence of out-of-focus sources (15). A set of two computer-controlled polarizing filters that could be rotated between each image collection was used to modulate lamp output. Excitation and emission filters were placed on two eight-position wheels that could be motorized independently under program control, making it possible to select a large number of relevant excitation/emission combinations. Four dichroic mirrors were adjusted on a Zeiss motorized slide, using an autocollimator to eliminate image shift resulting from inaccurate mirror positioning. All filters and dichroic mirrors were purchased from Omega Optical (Brattleboro, VT).

A Dage-MTI ISIT camera (Michigan City, IN), which is known to be sensitive to an illumination level of 5×10^4 lux, was used. Digital images were obtained at a resolution of 512 × 512 pixels at eight bits/pixel, providing 256 gray levels. One pixel corresponded to 16 μm in the image plane.

Image Processing

Image collection. The images were processed and analyzed with an IBAS 2000 image analyzer (Kontron, Eching, Federal Republic of Germany). This system uses a 486/66 MHz computer with 16 MB RAM and an MIAP 2 array processor with a 16 MB video memory and a real TV video board. The software was IBAS release 2.5. Sets of fluorescent images of the same field were collected sequentially with appropriate pairs of excitation/emission filters. To compensate for variations in brightness due to different dye efficiencies, the excitation intensity was adjusted for each image by the two rotating polarizing filters. After each image collection, a shutter in the excitation light path was closed to minimize dye bleaching. Sequence of illumination was used for all preparations, beginning with the longest wavelength at 660 nm and ending with the ultraviolet (UV) excitation at 365 nm. For each preparation, the voltage was adjusted to the highest value that gave no saturation in the brightest image (generally, the PE image) and was kept fixed for all sequential acquisitions of the same field in order to avoid image rotation. The black level was not removed electronically. An additional brightfield transmitted image was used for segmentation and as alignment reference. All images were recorded by averaging 100 frames for a total exposure time of about 4 s. Images were stored on disk for further analysis.

Selection and alignment of objects. The segmentation of objects from background was achieved by an interactive thresholding procedure, which was performed on the brightfield image. A CLOSE operation connected incomplete outlines. Particles that were too small or dirt particles were removed on the basis of their size (less than 30 pixels). Attached spots were separated by a THINBIN procedure, which was used to erode object outlines. Objects were then filled. Detected objects were displayed as binary masks and were identified. An automatic step was used to discard objects touching the edge of the image frame and, finally, to check the objects to be quantified. Because the available emission filters did not have strictly parallel faces, object shifts occurred at the different excitation/emission combinations. Therefore, sequential images of the same field were realigned interactively with the brightfield mask as reference.

Image restoration. The following corrections were performed on each image to ensure accurate fluorescence quantification. For shading correction, a set of reference images (one per filter set) was acquired that consisted of a drop of saline solution placed onto a Hamax slide. Each image was divided, pixel to pixel, by its reference and was multiplied by the mean gray level of the latter. Background correction was made by subtracting the modal value of the first peak of the gray level histogram obtained after shading correction. This value was considered to be a valid estimate of the field background, because it was unlikely to be influenced by cellular halos and impurities. The mean gray level originating from light reflected by the surface of unlabeled beads was also subtracted.

Image display and printing. The images shown in Figure 4 were obtained by converting the red, green, and blue images into .TIFF format and by exporting them to Photoshop software (Adobe, Mountain View, CA) for display on a PC screen and graphical sublimation printing. Following automatic compression, the images were stored on Bernouilli cassettes.

RESULTS

Development of Seven-Dye Immunophenotyping

Primary selection of probes and filter sets. Multiple immunophenotyping required careful fluorochrome selection. A spectrofluorometric evaluation of 14 dyes was first performed to identify a combination of dyes that could be spectrally resolved (Fig. 2, Table 1). When two probes were found to display approximately the same excitation and emission spectra, the less readily available probe was discarded: For this reason, FITC, PE, and APC were chosen in place of Bodipy, Cy3, and CPC, respectively. TxR gave a weak signal compared with its tandem with PE (Red613) and also was discarded. For the other pairs of spectrally close dyes (i.e., AMCA/CB and Red670/PerCP), selection could not be made from spectrofluorometric analyzes, and these had to be compared under image cytometry (see below).

Appropriate pairs of excitation and emission filters were selected to optimize excitation and light collection while minimizing the crosstalk between fluorophores (Table 2). Excitation filters for AMCA/CB and LY were set to match mercury emission lines at 365 and 405 nm, respectively; a single filter at 485 nm was sufficient for excitation of FITC, PE, Red613, Red670, and PerCP, even though excitation of PE and PE tandems by the 546 nm line of the mercury lamp resulted in a greater signal-to-noise ratio than at 485 nm (34). APC excitation was set at 590 nm, slightly below its absorption maximum, in an attempt to reduce overlap with Cy5. Finally, Cy5 excitation was placed at 660 nm. Emission filters were set near the emission maxima of their respective dyes, except for Cy5, which was measured above 700 nm to facilitate spectral resolution from APC.

Determination of crosstalk matrix by digital imaging cytometry. Microbeads labeled with saturating concentrations of the different conjugated dyes were used. Emission intensities of all fluorochromes were recorded under eight filter combinations, which are listed in Table 2. From these data, the crosstalk matrix of Table 3 was obtained. The columns indicate the fluorescence intensities recorded for each fluorochrome with the different filter sets; inversely, the rows record all dye emissions occurring through each of the filter combinations. This matrix, as shown below, served as the basic tool for both final dye selection and correction of spectral overlap.

Final selection of probes and filter sets. The matrix provided clear criteria with which to achieve a definitive dye selection. CB and AMCA could be both used as UV-excited dyes. Other investigators have reported the superiority of CB over AMCA in terms of quantum yield and resolution (40). However, with the 410/530 nm LY set, CB, AMCA, and LY had emission intensities of 8, 3, and 47 units, respectively, indicating that AMCA was resolved better than CB in the configuration used, whereas both dyes gave near identical emission efficiency with the 365/425 nm set.

In the near UV region, LY has an interesting spectrum. It has approximately the same emission as FITC at 530 nm, but its absorption band is located at the lower wavelength of 410 nm. Although it has a rather weak efficiency (4.7% of PE; see Table 3), LY excitation is ideally placed between that of AMCA and FITC. Therefore, LY was included in the fluorochrome combination.

In the group of 485 nm-excitable dyes, the most commonly used (FITC and PE) are easy to separate for two-color immunofluorescence. Additional probes (i.e., Red613, Red670, and PerCP) that were introduced initially for three- and four-color flow cytometry along with FITC and PE were evaluated in image cytometry. Although there is considerable overlap between the emissions of PE and Red613, the high signals provided by these two dyes allowed their spectral discrimination. PerCP was preferred to Red670, because its narrower emission spectrum facilitated its spectral discrimination from PE and Red613.

Among red-emitting dyes, APC and CY5 were compared in image cytometry. Cy5 has a greater proportion of its emission above 700 nm than APC, but these two dyes could not be resolved spectrally when they were used simultaneously. This was due to the fact that too many dyes (i.e., PE, Red613, PerCP, APC, and Cy5) were detected with the 590/660 nm filter set, and this led to a spectral compensation that was too complex. The solution implemented was to measure APC fluorescence with the 660/LP700 nm filter set, which was designed initially for Cy5, and to discard Cy5 from the probe combination. The spectra of the seven-dye combination that was selected with their respective excitation/emission filters are depicted in the left part of Figure 2.

Modulation of image intensity. Because of the limited dynamic range of the ISIT camera and also because better discrimination can be expected if all images have comparable brightness, it was necessary to modulate the source intensity with two rotating polarizing filters positioned in front of the mercury lamp. The source intensity could be reduced up to 100-fold by turning the planes of polarization from parallel to perpendicular (Table 4). The polarizing filters could be rotated between each image collection, making it possible to adapt the lamp output to each dye. The bright signals, especially those of PE, Red613, and PerCP, were attenuated, while the weaker signals of LY and APC were relatively amplified. Further amplification of AMCA and LY emissions would have been useful, but this option was limited by the high background in the UV region due to the strong intensities of the 365 and 405 nm lines of the mercury lamp and the insufficient blocking of the filters outside the mercury lines. Spectral overlap values recorded with relative amplification were consequently increased, whereas the other ones were attenuated. Therefore, a second spectral crosstalk matrix was acquired by using output modulation. All subsequent recordings using spectral overlap correction coefficients derived from this second matrix were performed under the same conditions of illumination adjustment (Table 4).

Automatic spectral compensation. A set of linear equations describing the mathematical relationships be-

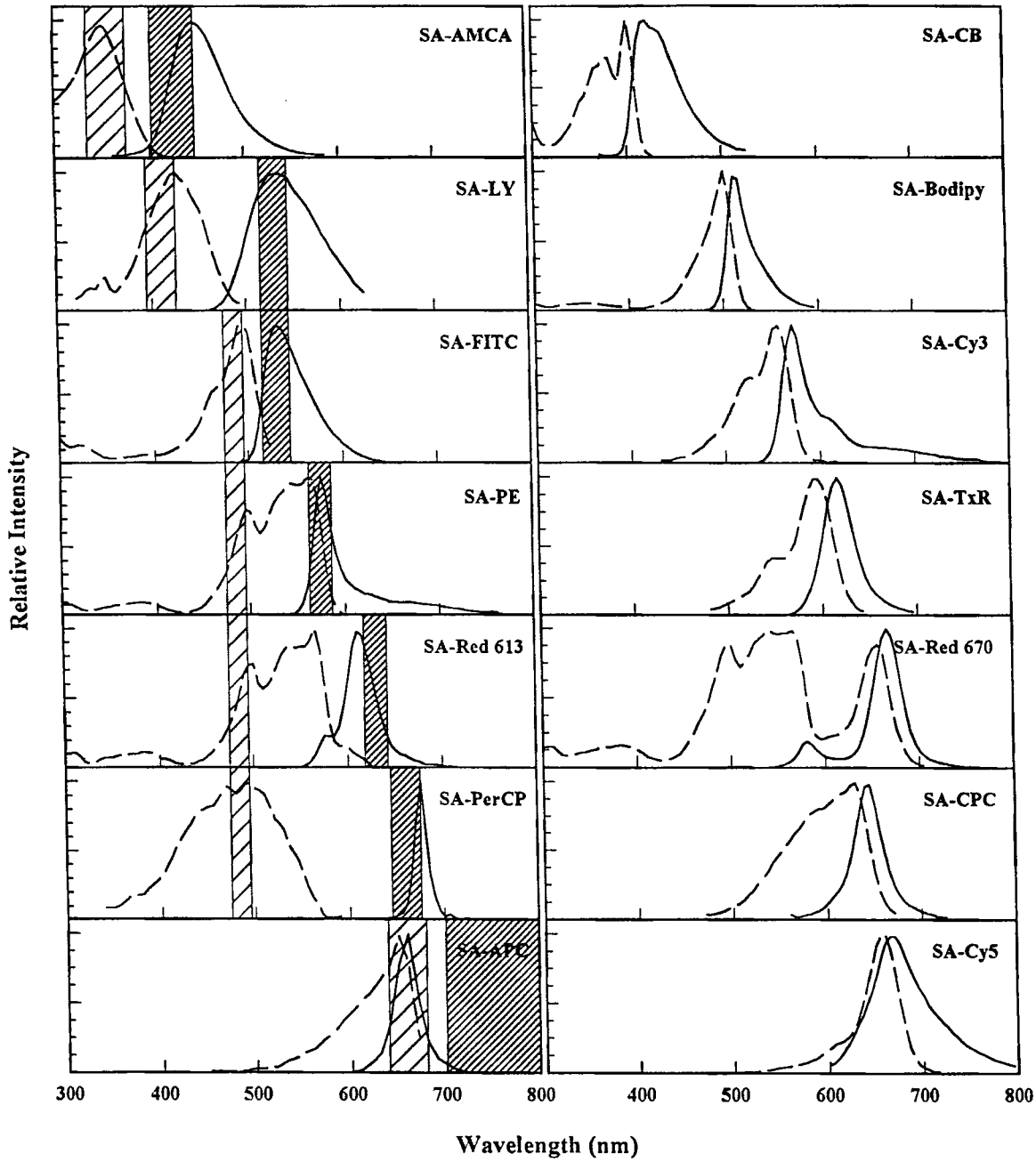

FIG. 2. Excitation (dashed line) and emission (solid line) spectra of 14 streptavidin-conjugated fluorochromes. Excitation/emission bandpasses are indicated by light and heavy hatching, respectively, for the seven dyes that were finally selected for multifluorescence imaging.

tween all dye emissions was derived from the spectral crosstalk matrix (see Appendix). The equations were introduced into the image restoration program following the shading and background correction steps. The resolution of these equations was applied numerically to the mean gray level within each data region to yield the corrected value of each object. Pixelwise combinations were also computed by using the COMBINE procedure of the IBAS software to display corrected images.

Evaluation of Seven-Dye Immunophenotyping

Fluorochrome fading. Compared with free output, the interposition of two polarizers in parallel directions reduced the source intensity to about 50%, which was useful to reduce dye fading. Rates of fading produced with this baseline output in all cases were less that 10% during the 4-s exposure used. These were further slowed down by output modulation, except for the APC channel,

Table 2
Filter Sets Designed for Initial Evaluation of Spectral Overlaps in the Ten-Dye Set[a]

	Wavelengths (nm)				
	Excitation			Emission	
Fluorescent probe	Center	Bandpass[b]	Dichroic (50%)[c]	Center	Bandpass
AMCA/CB	355	40	400	425	45
LY	405	10	510	530	30
FITC	485	22	510	530	30
PE	485	22	510	575	25
Red613	485	22	510	630	23
PerCP/Red670	485	22	510	660	32
APC[d]	590	45	620	660	32
Cy5/APC[d]	660	40	690	700	LP[e]

[a]All filters were interference filters from Omega Optical Inc., Brattleboro, VT. For fluorescent probe abbreviations, see Materials and Methods.
[b]Total bandpass at half maximum transmittance.
[c]Wavelength of half maximum transmittance.
[d]APC fluorescence was finally recorded with a 660/LP700 filter set in place of the 590/660 filter set (see text).
[e]This is a long-pass filter.

Table 3
Spectral Crosstalk Matrix for Initial Evaluation of the Ten-Dye and Filter Set[a]

	Mean emission intensity (arbitrary units)									
Filter sets (nm)[b]	CB	AMCA	LY	FITC	PE	Red613	PerCP	Red670	APC	Cy5
365/425	107	100	8							
410/530	8	3	47	16						
485/530			6	176	11					
485/575				43	1,000	102		40		
485/630					225	347		31		
485/660					75	162	416	556	5	
590/660					102	234	32	724	154	29
660/LP700[c]							14	52	39	40

[a]Ten dyes were measured in eight channels to evaluate their potential spectral resolution. All data are from streptavidin-conjugated fluorochromes bound to latex microbeads at saturation (for fluorochrome abbreviations, see Materials and Methods). Fluorescence intensities are expressed in arbitrary units relative to a value of 1,000 attributed to the fluorescence of PE at 575 nm. Columns indicate the fluorescence intensities of each probe recorded in all channels; rows record all dye emissions occurring through particular filter sets.
[b]Filter sets are indicated by the center wavelengths of excitation and emission bandpasses.
[c]This is a long-pass filter.

which was recorded without additional source attenuation. Fading was reversible in part during the period following exposure, when the beam was shifted out from the preparation. Another way to reduce the influence of fading on spectral crosstalk values was to use the same sequence of illumination, beginning with the lowest energy at 660 nm and ending with the highest one at 365 nm.

Precision and linearity of spectral compensation. Microbead suspensions coated with different concentrations of biotinylated IgG1 were labeled with the various dyes to obtain wide ranges of fluorescence intensities. They were visualized sequentially with each one of the filter combinations (Table 2). For each fluorochrome microbead, emissions measured with its own filter set were plotted against the emissions obtained with the other filter sets. An example of the spectral contaminations of PE-labeled beads is shown in Figure 3. The slopes of these curves indicate the percentage crosstalk of PE in other relevant emission filters, i.e., 630 nm for Red613 and 660 nm for PerCP/Red670. Similar measures were made for all possible dye and filter combinations. Accurate quantitative measurement of fluorescence intensities was checked by the stability of these crosstalk values when measured on a number of different fields. The CV of such repeated measurements was less than 6% for percentage crosstalk values above 10 and less than 9% for values between 3 and 10. The independence of spectral crosstalk from emission intensity values was ascertained by the linearity of these curves (correlation coefficient >0.90 in all cases). The accuracy of background and

Table 4
Spectral Crosstalk Matrix for the Selected Filter and Seven-Dye Set[a]

Filter sets (nm)[b]	Lamp output (adjustment factor)[c]	Mean emission intensity (arbitrary units) AMCA	LY	FITC	PE	Red613	PerCP	APC
365/425	0.46	46.6 (100)	3.6 (6)					
410/530	1.26	4.2 (9)	58.7 (100)	20.6 (17)				
485/530	0.70		4.3 (7)	123.3 (100)	8.1 (8)			
485/575	0.10			4.3 (3)	100 (100)	10.2 (8)		
485/630	0.35				78.9 (79)	121.5 (100)		
485/660	0.30				22.6 (23)	48.7 (40)	124.9 (100)	4 (1)
660/LP700[d]	2.90						40.4 (32)	111.7 (100)

[a]Data are from latex microbeads labeled at saturation with seven streptavidin-conjugated fluorochromes selected for multiparameter image cytometry (for fluorochrome abbreviations, see Materials and Methods). Spectral crosstalk values were measured under adaptation of lamp output to the brightness of each dye. Fluorescence intensities are expressed in arbitrary units relative to a value of 100 attributed to the fluorescence of PE at 575 nm. Columns indicate the fluorescence intensities of each probe recorded in all channels; rows record all dye emissions occurring through each of the filter sets. Figures in parentheses indicate percentage crosstalk values of each dye.
[b]Filter sets are indicated by the center wavelengths of excitation and emission bandpasses.
[c]Compared with data in Table 3, lamp output was multiplied by the factors indicated for each channel.
[d]This is a long-pass filter.

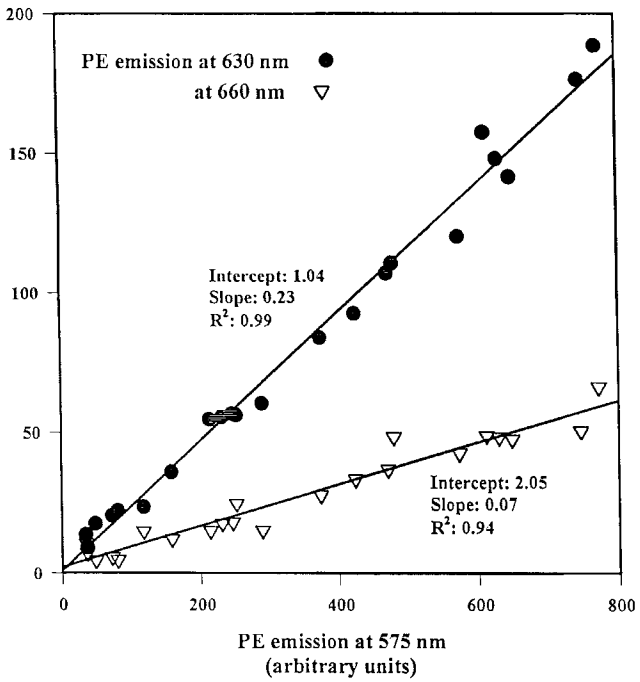

FIG. 3. Emission intensities of streptavidin-conjugated R-phycoerythrin (PE) bound to latex microbeads under three different filter sets. Latex particles were labeled with PE under various concentrations of biotinylated immunoglobulin (IgG)1 in order to obtain a wide range of fluorescence intensities. Excitation was at 485 nm in each case. Overlapping PE emissions in the PE-Texas red tandem Red613 and peridinin-chlorophyll-protein (PerCP) channels at 630 and 660 nm, respectively, are plotted vs. PE emission at 575 nm. Each point represents the mean gray level (in arbitrary units) of a single particle. The slopes of these curves correspond to the crosstalk values 225 and 75 listed in Table 3.

shading corrections was established by the intercept of the regression lines with the axis origin.

Accuracy of spectral compensation. To verify that correction of spectral overlap did not cause some particles to be classified erroneously as positive or negative, two series of experiments were made. First, each of seven bead suspensions was labeled with one different dye; then, all seven suspensions were mixed (Fig. 4A). The statistics of positive and negative objects, which are listed in Table 5, demonstrate the ability of the image cytometry system to detect accurately seven distinct probes in one field and to correct spectral contaminations originating from any of these probes. The legend to Figure 4A illustrates how the algorithm described in the Appendix performs the spectral correction. Second, two suspensions were labeled with several dyes: The first suspension was labeled with AMCA, FITC, Red613, and APC, and the second suspension was labeled with LY, PE, and PerCP. The two suspensions were then mixed together (Fig. 4B). Signal intensities corresponding to presence or absence of labeling are shown in Table 6. These data show that it is possible to identify multiple-labeled objects of different types on the same field. In addition, the S.D. of emission intensities recorded for negative objects provide a basis for determining the detection limit for each label.

DISCUSSION

This paper describes a methodology that is aimed at optimizing multiple immunophenotyping and applying it to the detection and measurement of seven SA-fluorochrome probes bound to latex microbeads. The main points of the strategy were 1) preliminary selection of fluorochromes and filter/mirror sets based on spectrofluorometric data of streptavidin-fluorochrome solutions, 2) determination of the spectral crosstalk matrix from cytometric measurement of labeled microbeads and reselection of separable probes, 3) modulation of source intensity in order to harmonize the brightness of images, 4) spectral compensation based on a set of linear equations derived from the modified crosstalk matrix, and 5)

Table 5
Digital Fluorescence Imaging of Latex Microbeads Single Labeled With Seven Streptavidin-Conjugated Dyes[a]

	Mean emission intensity (arbitrary units)				
	Positive objects			Negative objects	
Fluorochrome[b]	Mean	Min	Max	Mean	S.D.
AMCA	46.5	22	89	1.0	1.8
LY	59.0	42	95	−0.5	1.8
FITC	123.9	97	178	1.2	2.2
PE	100.9	39	138	0.2	0.8
Red613	120.5	79	153	0.3	2.1
PerCP	126.8	88	189	1.6	2.4
APC	113.1	65	177	1.3	2.9

[a]Data from several fields (n = 87 beads) of the preparation depicted in Figure 4A were listed out in each fluorescence channel after background and spectral overlap correction. Each object was considered to be positive in the fluorescence channel where it had the highest gray level and was considered to be negative in the six others. Statistics of positive and negative beads are indicated for each type of labeling. *P* values for unpaired t tests between positive and negative objects were <0.0001 for all fluorochromes.
[b]For fluorochrome abbreviations, see Materials and Methods.

Table 6
Digital Fluorescence Imaging of Latex Microbeads Multiple Labeled With Seven Streptavidin-Conjugated Dyes[a]

	Mean emission intensity (arbitrary units)				
	Positive objects			Negative objects	
Fluorochrome[b]	Mean	Min	Max	Mean	S.D.
AMCA	34.2	27	50	1.5	0.9
LY	30.0	24	39	1.5	2.3
FITC	59.0	48	73	0.1	0.6
PE	47.6	36	62	1.4	1.6
Red613	56.6	44	78	−1.1	1.4
PerCP	58.5	43	75	3.7	2.2
APC	26.0	19	38	−2.8	1.4

[a]Data from several fields (n = 30) of the preparation illustrated in Figure 4B were listed out in each fluorescence channel. Each object could be attributed to one of two populations: The first one was labeled with AMCA, FITC, Red613, and APC and was negative for LY, PE, and PerCP, and the second one was labeled with LY, PE, and PerCP but was negative for AMCA, FITC, Red613, and APC. Statistics of emission values corresponding to presence or absence of labeling are indicated in each probe channel. *P* values for unpaired t tests between positive and negative objects were <0.0001 for all fluorochromes.
[b]For fluorochrome abbreviations, see Materials and Methods.

evaluation of accuracy and sensitivity of the procedure. The strategy was iterative, because steps 2–5 were repeated until satisfactory discrimination was achieved.

Because, when "n" markers are used simultaneously, the number of potential combinations of positive and negative probe emissions is 2^n, it may be necessary to analyze a few hundred cells to get significant population statistics. The maximum number of analyzable particles in one field is about 50 with the ×40 objective used in this study; therefore, several fields of the same preparation would have to be collected in a seven- parameter phenotyping study. To rapidly analyze larger samples, the wider field of view provided by a reducing camera lens would be required. For instance, a ×0.63 ocular lens could multiply both the light gathering power of the optical system and the viewing area by a factor of about 2.5.

To ensure the stability of spectral compensation, the ISIT camera was used at constant gain, a procedure that considerably limited its interscene dynamic range. Keeping the fluorescence of the seven probes on scale was made possible by tuning the excitation intensity with two polarizers for each dye collection. However, although excitation adjustment can extend the interscene dynamic range of the camera, this procedure does not affect its capacity to record widely variable emission intensities within a given field, i.e., its intrascene dynamic range (38). In cases where, in a given field, strongly labeled cells emit a saturating nonquantifiable signal (whereas some others give a barely detectable one), two methods may be proposed to extend the usable dynamic range available with the ISIT camera, whose range is intrinsically limited by its eight-bit gray level scale. First, two images recorded at low and high illumination may be merged after calculating a corrected intensity on each cell. Second, a double recording can be dispensed with if a camera with a much wider dynamic range, such as a 12–16 bit CCD camera, is used.

Based on the strategy developed in this study and the available equipment, we found that seven SA fluorochromes can be discriminated and measured. However, this is by no means the maximal number of probes that can be used in the context of immunophenotyping applications. For instance, utilization of Cy7 would only require a camera with sufficient sensitivity in the infrared region (31). Detection of propidium iodide-stained cells using a 360/620 filter set may be indispensable to ensure viability of the cells to be immunophenotyped and would be compatible with the dye combination used in this study. Europium chelates also have large Stokes shifts (29) and may have applications in the future.

Previous works have reported successful discrimination of seven probes by combinatorial analysis. These studies used probes labeled with mixtures of three dyes that were combined to provide up to seven color combinations (20,25). Combinatorial analysis is applicable when a given site (for instance, a chromosomal segment) will bind only one specific fluorescent probe. In the techniques described here, each cellular marker has to be labeled with a distinct fluorochrome, because a given cellular target may possibly be occupied by several antigens.

The application of the methodology developed here to cell labeling has several implications. It would be advisable to conjugate the weakest fluorophores to the antibodies that are expected to yield the strongest labeling. The amplification provided by indirect labeling via biotin-streptavidin or antiisotype can also help to increase the detection of these less intense fluorophores. Cellular preparations can also show a higher background in the

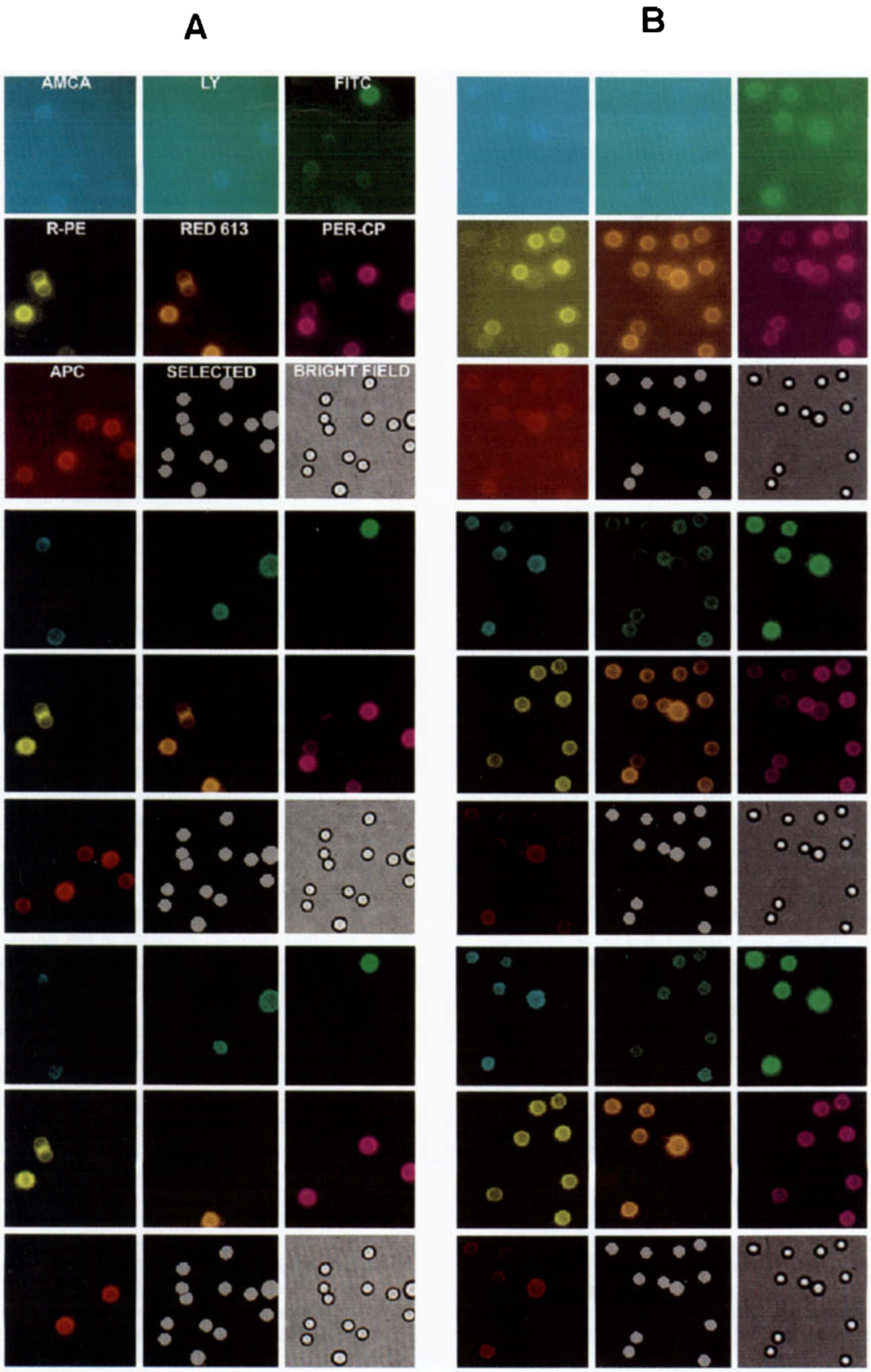

FIG. 4. (Legend on facing page)

AMCA, LY, and FITC channels because of autofluorescence. Unless the latter can be eliminated from the cell preparation, it must be corrected by using digital imaging methods, such as subtracting the mean fluorescence ±3 S.D. determined on a negative control preparation. An additional consideration is the large variability of cellular antigen density, which may span up to four orders of magnitude of fluorescence intensity. Therefore, the wide dynamic range provided by CCD cameras may be required in order to permit accurate quantification and correction of cellular signals.

Multiple parameter phenotyping will certainly help to assess complex phenotypes in a single-labeling procedure, especially when one or several probes are expected to react with a small percentage of the population of interest. In such cases, it may be difficult to find unequivocal relationships from a series of two- or three-color labelings. This technique can also prove to be useful for the phenotyping of small samples, such as hemopoietic colonies in the early stages of their development. In many cases, the need for large cell numbers by flow cytometers may lead to a severe limitation of the numbers of usable probes. Image cytometry, however, requires only a few thousand cells to perform such an analysis.

ACKNOWLEDGMENTS

The authors are grateful to Prof. C. Houssier and his team from the Department of Physical Chemistry, University of Liege, for excellent assistance in spectrofluorometric measurements and M.Y. de Menten (Zeiss, Brussels, Belgium) for help in the development of the IBAS programs.

FIG. 4. Multiparameter fluorescence imaging of seven fluorochromes bound to latex microbeads. Image processing of a relevant field of two distinct preparations are displayed. **A:** Seven bead suspensions were labeled with aminomethylcoumarin acetate (AMCA), Lucifer yellow (LY), fluorescein isothiocyanate (FITC), PE, Red613, PerCP, or allophycocyanin (APC), and aliquots were mixed in a single suspension. **B:** Microbeads were stained either with AMCA, FITC, Red613, and APC or with LY, PE, and PerCP and were mixed in a single suspension. For each field, seven fluorescent images were acquired by using the filter sets depicted in Figure 2. They are indicated by their corresponding fluorochromes. The image termed "selected" represents the binary masks of objects to be quantified. The brightfield transmitted image is also displayed. All sets of nine images are displayed in the same order. Image processing is depicted in three steps. Fluorescent images are displayed without image correction (top set of nine squares), after background and shading correction (middle set of nine squares), and after the COMBINE procedures used to correct for spectral overlaps (bottom set of nine squares). To illustrate the algorithm used by the spectral compensation routine, consider the middle and bottom sets in A. The equations for correction of PE, Red613, PerCP, and APC emissions are Equations 4–7 in the Appendix. Note that the three $PE^+/Red613^+$ cells shown in the middle set are found to be $PE^+/Red613^-$ in the corrected bottom set, because Equation 5 for Red613 contains a term (−0.85 Em4) that subtracts a fraction of measured PE emission from measured Red613 emission. Similarly, a $PE^-/Red613^+/PerCP^+$ cell in the middle set is found to be positive for Red613 only after correction (bottom set). Of the several cells in the PerCP and APC images in the middle set, three are $PerCP^+$, and two are APC^+ after correction in the bottom set.

LITERATURE CITED

1. Afar B, Merrill J, Clark EA: Detection of lymphocyte subsets using three-color/single-laser flow cytometry and the fluorescent dye peridinin chlorophyll-a protein. J Clin Immunol 11:254–261, 1991.
2. Aubry JP, Durand I, De Paoli P, Banchereau J: 7-Amino-4-methylcoumarin-3-acetic acid-conjugated streptavidin permits simultaneous flow cytometry analysis of either three cell surface antigens or one cell surface antigen as a function of RNA and DNA content. J Immunol Methods 128:39–49, 1990.
3. Bagwell CB, Adams EG: Fluorescence spectral overlap compensation for any number of flow cytometry parameters. Ann NY Acad Sci 677:167–184, 1993.
4. Beavis AJ, Pennline KJ: Simultaneous measurement of five cell surface antigens by five-colour immunofluorescence. Cytometry 15: 371–376, 1994.
5. Campana D, Pui CH: Detection of minimal residual disease in acute leukemia: Methodologic advances and clinical significance. Blood 85:1416–1434, 1995.
6. Champaneria S, Swenarchuk LE, Anderson MJ: Increases in pericellular proteolysis at developing neuromuscular junctions in culture. Dev Biol 149:261–277, 1992.
7. Civin CI: Human monomyeloid cell membrane antigens. Exp Hematol 18:461–467, 1990.
8. DeBiasio R, Bright GR, Ernst LA, Waggoner AS, Taylor DL: Five-parameter fluorescence imaging: Wound healing of living Swiss 3T3 cells. J Cell Biol 105:1613–1622, 1987.
9. Debili N, Issaad C, Massé JM, Guichard J, Katz A, Breton-Gorius J, Vainchenker W: Expression of CD34 and platelet glycoproteins during human megakaryocytic differentiation. Blood 80:3022–3035, 1992.
10. Glazer AN, Stryer L: Phycofluor probes. Trends Biochem Sci 9:423–427, 1984.
11. Gore SD, Kastan MB, Civin CI: Normal human bone marrow precursors that express terminal deoxynucleotidyl transferase include T-cell precursors and possible lymphoid stem cells. Blood 77:1681–1690, 1991.
12. Greimers R: Contribution à l'analyse multiparamétrique par cytométrie en flux de lymphomes radio-induits chez la souris et de tumeurs solides humaines. Doctoral Thesis, University of Liège. Presses Universitaires, Liège, 1993, pp 1–441.
13. Greimers R, Trebak M, Moutschen M, Jacobs N, Boniver J: Improved four-color flow cytometry method using fluo-3 and a triple immunofluorescence for analysis of intracellular calcium ion ($[Ca^{2+}]i$) fluxes among mice lymph node B and T lymphocyte subsets. Cytometry 23:205–217, 1996.
14. Haugland RP, Larison KD: Handbook of Fluorescent Probes and Research Chemicals. Molecular Probes, Inc., Eugene, OR, 1992, pp 1–421.
15. Inoue S: Imaging of unresolved objects, superresolution, and precision of distance measurements with videomicroscopy. Methods Cell Biol 30:85–112, 1989.
16. Khalfan H, Abuknesha R, Rand-Weaver M, Price RG, Robinson D: Aminomethyl coumarin acetic acid: A new fluorescent labeling agent for proteins. Histochem J 18:497–499, 1986.
17. Loken MR, Shah VO, Dattilio KL, Civin CI: Flow cytometric analysis of human bone marrow. II. Normal B lymphocyte development. Blood 70:1316–1324, 1987.
18. Mayani H, Lansdorp PM: Thy-1 expression is linked to functional properties of primitive hematopoietic progenitor cells from human umbilical cord blood. Blood 83:2410–2417, 1994.
19. Mehrotra B, George TI, Kavanau K, Avet-Loiseau H, Moore D II, Willman CL, Slovak ML, Atwater S, Head DR, Pallavicini MG: Cytogenetically aberrant cells in the stem cell compartment ($CD34^+lin^-$) in acute myeloid leukemia. Blood 86:1139–1147, 1995.
20. Nederlof PM, van der Flier S, Wiegant J, Raap AK, Tanke HJ, Ploem JS, van der Ploeg M: Multiple fluorescence in situ hybridization. Cytometry 11:126–131, 1990.
21. Oi VT, Glazer AN, Stryer L: Fluorescent phycobiliprotein conjugates for analyses of cells and molecules. J Cell Biol 93:981–986, 1982.
22. Olweus J, Lund-Johansen F, Terstappen LWMM: CD64/FcγRI is a

granulo-monocytic lineage marker on $CD34^+$ hematopoietic progenitor cells. Blood 85:2402–2413, 1995.
23. Paulus JM, Grosdent JC, de Menten Y: Four wavelength immunofluorescence using an image analyzer: A preliminary evaluation. Seventh Meeting Belgian Hematol Soc, Brussels, pg. 52, 1992 (abstract).
24. Perkampus HH: UV-VIS Spectroscopy and Its Applications. Springer-Verlag, Berlin, 1992, pp 1–244.
25. Ried T, Baldini A, Rand TC, Ward DC: Simultaneous visualization of seven different DNA probes by in situ hybridization using combinatorial fluorescence and digital imaging microscopy. Proc Natl Acad Sci USA 89:1388–1392, 1992.
26. Riggs JL, Seiwald RJ, Burckhalter JH, Downs CM, Metcalf TG: Isothiocyanate compounds as fluorescent labeling agents for immune serum. Am J Pathol 34:1081–1097, 1958.
27. Roederer M, Bigos M, Nozaki T, Stovel RT, Parks DR, Herzenberg LA: Heterogeneous calcium flux in peripheral T cell subsets revealed by five-color flow cytometry using log-ratio circuitry. Cytometry 21: 187–196, 1995.
28. Schlossman SF, Boumsell L, Gilks W, Harlan JM, Kishimoto T, Morimoto C, Ritz J, Shaw S, Silverstein R, Springer T, Tedder TF, Todd RF: Leucocyte Typing V: White Cell Differentiation Antigens. Oxford University Press, Oxford, 1995, pp 1–2044.
29. Seveus L, Väisälä M, Syrjänen S, Sandberg M, Kuusisto A, Harju R, Salo J, Hemmilä I, Kojola H, Soini E: Time-resolved fluorescence imaging of europium chelate label in immunohistochemistry and in situ hybridization. Cytometry 13:329–338, 1992.
30. Shapiro HM: Practical Flow Cytometry, 3rd Ed. Wiley-Liss, New York, 1995, p 214.
31. Southwick PL, Ernst LA, Tauriello EW, Parker SR, Mujumdar RB, Mujumdar SR, Clever HA, Waggoner AS: Cyanine dye labeling reagents—Carboxymethylindocyanine succinimidyl esters. Cytometry 11:418–430, 1990.
32. Srour EF, Leemhuis T, Jenski L, Redmond R, Jansen J: Cytolytic activity of human natural killer cell subpopulations isolated by four-color immunofluorescence flow cytometric cell sorting. Cytometry 11:442–446, 1990.
33. Srour EF, Leemhuis T, Brandt JE, vanBesien K, Hoffman R: Simultaneous use of rhodamine 123, phycoerythrin, Texas red, and allophycocyanin for the isolation of human hematopoietic progenitor cells. Cytometry 12:179–183, 1991.
34. Steen HB: Characteristics of flow cytometers. In: Flow Cytometry and Sorting, Melamed MR, Lindmo T, Mendelsohn ML (eds). Wiley-Liss, New York, 1990, pp 11–25.
35. Stewart WW: Lucifer dyes—Highly fluorescent dyes for biological tracing. Nature 292:17–21, 1981.
36. Terstappen LWMM, Huang S, Safford M, Lansdorp PM, Loken MR: Sequential generations of hematopoietic colonies derived from single nonlineage-committed $CD34^+$, $CD38^-$ progenitor cells. Blood 77:1218–1227, 1991.
37. Titus JA, Haugland RP, Sharrow SO, Segal DM: Texas red, a hydrophilic, red-emitting fluorophore for use with fluorescein in dual parameter flow microfluorometric and fluorescence microscopic studies. J Immunol Methods 50:193–204, 1982.
38. Waggoner A, DeBiasio R, Conrad P, Bright GR, Ernst L, Ryan K, Nederlof M, Taylor D: Multiple spectral parameter imaging. Methods Cell Biol 30:449–478, 1989.
39. Waggoner AS, Ernst LA, Chen CH, Rechtenwald DJ: A new fluorescent antibody label for three-color flow cytometry with a single laser. Ann NY Acad Sci 677:185–193, 1993.
40. Whitaker JE, Haugland RP, Moore PL, Hewitt PC, Reese M, Haugland RP: Cascade blue derivatives: Water soluble, reactive, blue emission dyes evaluated as fluorescent labels and tracers. Ann Biochem 198: 119–130, 1991.

APPENDIX: CALCULATION OF SPECTRAL OVERLAP CORRECTIONS

The determination of the fluorescence intensities of each of the seven dyes requires the resolution of a set of seven linear equations in seven unknowns and is an application of multicomponent analysis (24). The *unknowns* (F1 . . . F7) are the actual emissions of AMCA, LY, FITC, PE, Red613, PerCP, and APC, respectively, when cleared of crosstalk from the others. The *measures* (Em1 . . . Em7) are the total emissions originating from any fluorochrome and detected within each filter set (see Table 4). The system can be written as the following equations:

$$\begin{aligned}
Em1 &= F1 + b1\,F2 + c1\,F3 + d1\,F4 + e1\,F5 + f1\,F6 + g1\,F7\\
Em2 &= a1\,F1 + F2 + c2\,F3 + d2\,F4 + e2\,F5 + f2\,F6 + g2\,F7\\
Em3 &= a2\,F1 + b2\,F2 + F3 + d3\,F4 + e3\,F5 + f3\,F6 + g3\,F7\\
Em4 &= a3\,F1 + b3\,F2 + c3\,F3 + F4 + e4\,F5 + f4\,F6 + g4\,F7\\
Em5 &= a4\,F1 + b4\,F2 + c4\,F3 + d4\,F4 + F5 + f5\,F6 + g5\,F7\\
Em6 &= a5\,F1 + b5\,F2 + c5\,F3 + d5\,F4 + e5\,F5 + F6 + g6\,F7\\
Em7 &= a6\,F1 + b6\,F2 + c6\,F3 + d6\,F4 + e6\,F5 + f6\,F6 + F7
\end{aligned}$$

The coefficients a1–a6 . . . g1–g6 represent the crosstalks of a particular dye in adjacent filter sets. For instance, d3 is the fraction of the fluorescence of FITC at 530 nm that can be detected at 575 nm. These coefficients were measured experimentally under standardized conditions of lamp intensity and exposure times, and many of these were found to be equal to zero (see Table 4). By using percentage crosstalk values, the set of equations can be rewritten in a much simpler way:

$$\begin{aligned}
Em1 &= F1 + 0.06\,F2\\
Em2 &= 0.09\,F1 + F2 + 0.17\,F3\\
Em3 &= 0.07\,F2 + F3 + 0.08\,F4\\
Em4 &= 0.03\,F3 + F4 + 0.08\,F5\\
Em5 &= 0.79\,F4 + F5\\
Em6 &= 0.23\,F4 + 0.40\,F5 + F6 + 0.01\,F7\\
Em7 &= 0.32\,F6 + F7
\end{aligned}$$

or in matrix form:

$$\begin{bmatrix}
1 & 0.06 & 0 & 0 & 0 & 0 & 0\\
0.09 & 1 & 0.17 & 0 & 0 & 0 & 0\\
0 & 0.07 & 1 & 0.08 & 0 & 0 & 0\\
0 & 0 & 0.03 & 1 & 0.08 & 0 & 0\\
0 & 0 & 0 & 0.79 & 1 & 0 & 0\\
0 & 0 & 0 & 0.23 & 0.40 & 1 & 0.01\\
0 & 0 & 0 & 0 & 0 & 0.32 & 1
\end{bmatrix} \cdot \begin{bmatrix} F1\\ F2\\ F3\\ F4\\ F5\\ F6\\ F7 \end{bmatrix} = \begin{bmatrix} Em1\\ Em2\\ Em3\\ Em4\\ Em5\\ Em6\\ Em7 \end{bmatrix}$$

which in simplified form is written:

$$A \cdot X = Y.$$

The unknowns of vector X can be solved by the equation:

$$X = A^{(-1)}.Y,$$

where $A^{(-1)}$ is the following inversed matrix of A.

1.01	−0.06	0.01	0	0	0	0
−0.09	1.02	−0.17	0.01	0	0	0
0	−0.07	1.02	−0.09	0	0	0
0	0	−0.03	1.07	−0.09	0	0
0	0	0.03	−0.85	1.07	0	0
0	0	0	0.10	−0.41	1	−0.01
0	0	0	−0.03	0.13	−0.33	1

The inverse matrix can be written as a set of linear equations, which can be resolved by image processing to yield corrected emission intensity values.

$$F1 = 1.01\,Em1 - 0.06\,Em2 + 0.01\,Em3 \quad (1)$$

$$F2 = -0.09\,Em1 + 1.02\,Em2 - 0.17\,Em3 + 0.01\,Em4 \quad (2)$$

$$F3 = -0.07\,Em2 + 1.02\,Em3 - 0.09\,Em4 \quad (3)$$

$$F4 = -0.03\,Em3 + 1.07\,Em4 - 0.09\,Em5 \quad (4)$$

$$F5 = 0.03\,Em3 - 0.85\,Em4 + 1.07\,Em5 \quad (5)$$

$$F6 = 0.10\,Em4 - 0.41\,Em5 + Em6 - 0.01\,Em7 \quad (6)$$

$$F7 = -0.03\,Em4 + 0.13\,Em5 - 0.33\,Em6 + Em7 \quad (7)$$